

# Numerical Evaluation of Slender Glass Panel with Complex Geometry Subjected to Static Load and Soft-body Impact

Marcin Kozłowski<sup>1\*</sup>

<sup>1</sup> Department of Structural Engineering, Silesian University of Technology, Akademicka 5, 44-100 Gliwice, Poland

\* Corresponding author, e-mail: [marcin.kozlowski@polsl.pl](mailto:marcin.kozlowski@polsl.pl)

Received: 10 March 2021, Accepted: 16 April 2021, Published online: 28 April 2021

## Abstract

Current standards and glass codes of design practice require that glazing used in architectural applications has to be resistant to, in addition to typical loads, also accidental events, in particular human impact, without showing damage that is disproportionate to the original cause. A case study was performed of an indoor glass lantern in a public building made from slender two-side supported glass panels with a complex geometry (36 ventilation holes). The paper provides structural assessments and results of in-situ experiments including static loading and soft body impact. Results from numerical simulations of impact loading on the glass panels complementing the experimental results are also presented.

## Keywords

structural glass, laminated glass, experiments, numerical simulations, static loading, impact loading

## 1 Introduction

Current standards and glass codes of design practice require that glazing used in architectural applications has to be resistant to, in addition to static loads, also accidental events, in particular such as human impact, without showing damage that is disproportionate to the original cause [1–3].

Slender glass panels are widely used to build storefronts and indoor separation walls in offices, shopping malls and public buildings [4, 5]. The design and construction of such panels should be safe for general use and should meet current and accepted technical standards. This relates particularly to the situations where such panels are required to ensure protection of neighboring walkways and have to bear the loads of persons leaning against the glass. To meet these requirements, the panels are usually made of laminated glass which shows improved post-breakage performance [6, 7]. In case of breakage of a single sheet in the laminated glass, the interlayer prevents the fragments from being scattered. Therefore, the solution provides a certain level of residual load-bearing capacity and reduces the risk of injury from cuts.

With respect to the building standard EN 1991-1-1 [8], glass panels mounted vertically should satisfy the basic load requirements in terms of an internal or external wind load and a static barrier loading (crowd loads). The panels

should also protect people from cutting and piercing injuries resulting from accidental impacts. In addition, at risk areas, for instance at locations where a difference in height constitutes a falling risk, building codes require the use of safety glass, which performance and classification is assessed by the impact pendulum test according to EN 12600 [9].

The paper presents a case study of an indoor glass lantern in a public building constructed with slender glass panels with complex geometry previously reported in [5]. It briefly reports the structural assessment and results of in-situ testing including static loading and soft-body impact. The current paper is an extension of the contribution [5], it focuses on numerical studies aimed at better understanding of structural behavior of the panels under soft-body impact, in particular, the structural response in post-breakage state.

## 2 Case study

The lantern which is a subject of the case study allows natural sunlight to illuminate the underground stories of the building. It is also a part of the ventilation and smoke extraction system in the event of fire. This is reflected in the construction details, a number of holes located in the

lower part of the glass panels allows for efficient air flow between the interior floors and the lantern (Fig. 1). The lantern runs through several stories of the building, however, the glass panels that build the lantern span between two floors and are considered as separate components.

The glass panels create a glass room with an approximately height of 4.4 m and  $15 \times 6 \text{ m}^2$  in plan. Each glass panel with the dimensions of  $0.99 \times 4.38 \text{ m}^2$  consists of two 10 mm thick and fully toughened safety glass sheets laminated with 1.52 mm thick interlayer of Polyvinyl Butyral (PVB) [10]. The gap between panels is 10 mm.

In the lower part of the panels there is an array of  $6 \times 6$  ventilation holes, each being 50 mm in diameter. The spacing between the holes is 125 mm (center to center) in both directions. The array of holes starts at about 350 mm above the bottom edge and is located at about 180 mm from the vertical edge. The panels are self-supported along the bottom edge and through two nylon bearing blocks. Out-of-plane restraints are provided by the aluminum profiles through rubber gaskets.

According to design documentation, the panels have been designed for several load cases. These included an internal pressure of  $0.2 \text{ kN/m}^2$  and a barrier loading of  $1.0 \text{ kN/m}$  applied at the height of 1.1 m above the floor level. Although the structural design was proven to meet the requirements regarding maximum stress in glass and deflection, a decision was made to experimentally verify

the panels regarding the load-bearing capacity under static and soft-body impact loading. It was decided that two panels of the lantern were designated for in-situ destructive testing after which the elements would be replaced.

### 3 In-situ test set-up and main results

#### 3.1 Static barrier loading

A Single static barrier loading test was performed with respect to the loads according to EN 1991-1-1 [8]. The horizontal loading was applied at the height of 1.1 m above the finished floor level by a hydraulic jack mounted on a steel beam temporarily fixed to steel columns located at the corners of the lantern (Fig. 2). To ensure that the loading was applied as a linear load, a 100 mm wide flat steel bar 15 mm in thickness was bonded to the glass with epoxy resin, distributing the point load generated by the jack into a line load.

The vertical deflection of the panel was measured with a linear variable differential transformer (LDVT) that was installed centrally on the panel (on the hydraulic jack side) approximately 100 mm below the load introduction point. In addition, a set of single-axis strain gauges were bonded vertically to the panel at several positions on the tensile side of the glass to measure tensile strain. The locations of the gauges on the panel allowed for measurements of strains in the highest stressed area and analysis of the influence of the holes in the glass on the strain values. The location of the LDVT and the strain gauges are shown in Fig. 3.

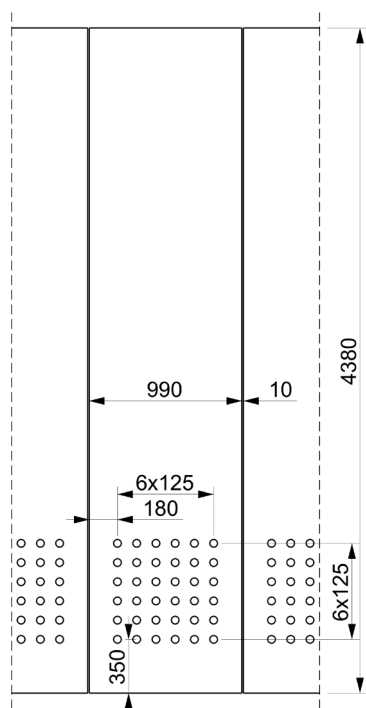


Fig. 1 Panel geometry (dimensions in mm)



Fig. 2 Static barrier loading test-set up

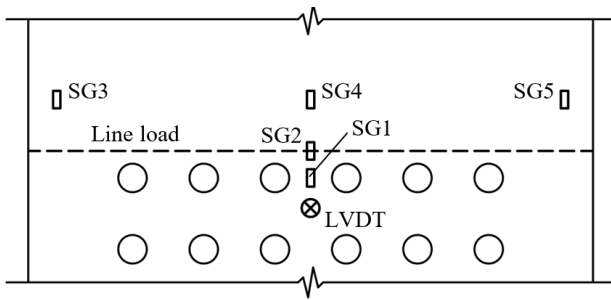


Fig. 3 Positions of strain gauges and LVDT

Fig. 4 shows the load versus displacement curve obtained from the static test. In the figure, local jumps of the signal can be observed. It is due to the fact that the load was powered by a hand pump which is usually used during in-situ tests. Under the characteristic designed load (1 kN/m) the measured deflection was approximately 30 mm. It should be noted that the location of the maximum deflection of the panel was above the load introduction point (at approximately 2.5 m from the finish floor level). The maximum deflection measured with a line ruler (34 mm) was lower than the allowed deflection as specified by the standard [2] that is  $4380/100 = 43.8$  mm.

Fig. 5 shows tensile stresses (in vertical direction) calculated from the strain gauges (Fig. 3). The stresses were calculated by multiplying the micro-strains by the Young's modulus of glass of 70 GPa assumed after material product standard [11]. It is clear, that the gauge no. 1 shows approximately 40 % higher values of stress than the gauges no. 2–5. It is due to the influence of holes in the glass resulting in stress concentrations in this area. The stress measured by the gauges no. 3-5 positioned 100 mm above the load introduction point show stresses lower about 7 % in comparison to the readings by the gauge no. 2.

### 3.2 Soft-body impact

Soft-body impact test was performed on a panel adjacent to the panel subjected to static barrier loading (Fig. 6). The impactor used was the pendulum described in [9] with a mass of 50 kg. It consisted of two pneumatic tires inflated with 4 bar air pressure and a steel weight. The impactor was brought to a drop height of 900 mm (the maximum value of drop height according to [2]) and released. The panel was hit at three locations: at the center of the set of holes, at the center at the height of 1500 mm and close to the edge at the height of 1500 mm. Despite considerable deflection of the panel after impact, no breakage of glass occurred. During the tests, no strain or deflection measurements were made.

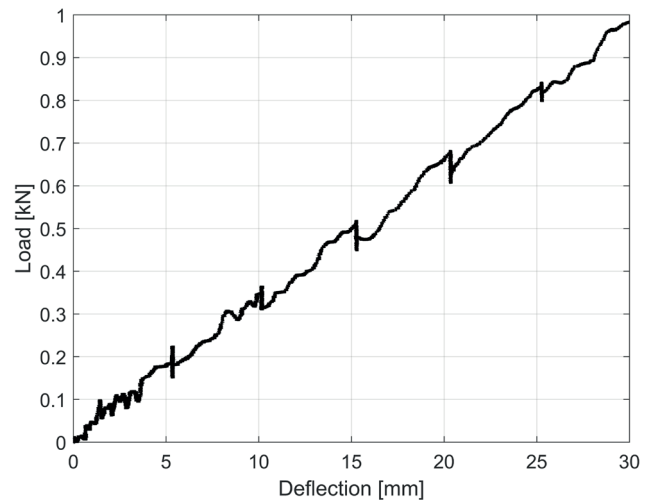


Fig. 4 Results of static loading test: Load vs. lateral displacement

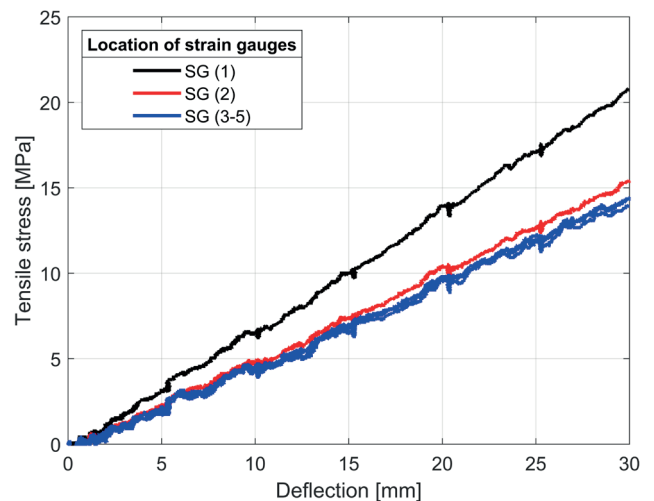


Fig. 5 Results of static loading test: Load vs. tensile stress

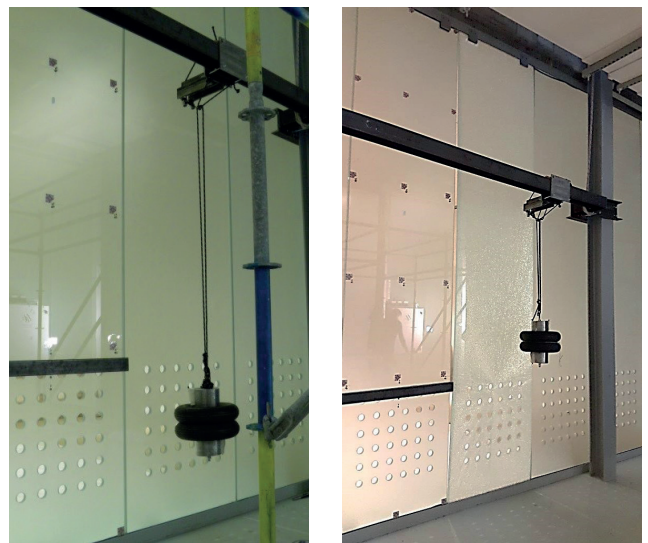


Fig. 6 Soft-body impact test-set up with: intact panel (left), panel with single ply deliberately fractured

In the next phase, the compressed ply of the laminated glass was deliberately fractured using a steel chisel and a hammer. The fractured ply was located on the impactor's side due to the fact that building users had no access to the interior of the lantern. The test was repeated with the drop height reduced to 450 mm (the lowest value of drop height according to [2]). It is common practice to use reduced values of loads in accidental load cases. During the test, the undamaged ply in the laminate remained intact which confirmed the safety of the panel in post-breakage state.

#### 4 Finite element modelling

A finite element (FE) model was developed using the commercial FE program ABAQUS [12] to further study the structural behavior of the panel with the same geometry and build-up as in the in-situ experiments. The study was aimed at better understanding the structural performance of the glass panel under static loading and soft-body impact, in particular in terms of its safety and utilization level. All analyses were run in displacement control including nonlinear effects of large deformations. The static and dynamic analyses of the panel were computed with Implicit Standards and Implicit Dynamic solvers [12], respectively.

The geometry and boundary conditions of the model are shown in Figs. 7 and 8. The panel was supported laterally along the top and bottom edges, whereas only the bottom edge was supported vertically. Two loading conditions were considered. The static barrier load was applied as liner loading 1 kN/m at 1.1 m above the bottom edge (Fig. 2). For the simulations of soft-body impact, a numerical model of impactor developed in [3] was used. The model consisted of two pneumatic tires and a steel rim with a total mass of 50 kg according to [9].

The set-up of the soft-body impact model is shown in Fig. 9. The swing of the pendulum was simulated by setting it in motion with the initial velocity  $v_0$  calculated for a given drop height ( $h$ ) with  $g = 9.81 \text{ m/s}^2$  according to Eq. (1):

$$v_0 = \sqrt{2gh} . \tag{1}$$

According to [2], various drop heights were considered (450, 700 and 900 mm). The values correspond to the impact energies of 220.7, 343.4 and 441.4 J, respectively.

Eight-node continuum shell finite elements (SC8R elements from ABAQUS elements library [12]) were used for the glass and interlayer. The continuum shell finite elements, just like regular shell elements, have only displacement degrees of freedom and the thickness is interpreted from the geometry of an element [12]. The continuum

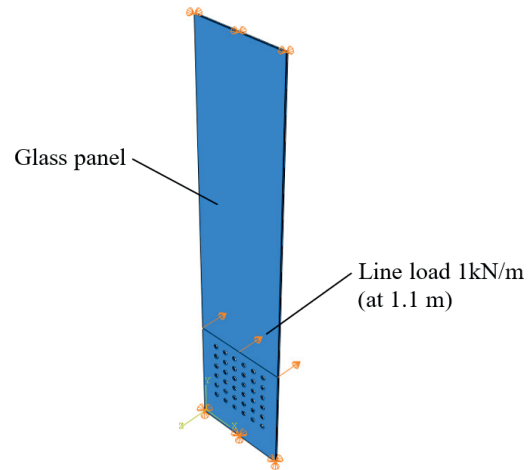


Fig. 7 Finite element model used for static barrier loading

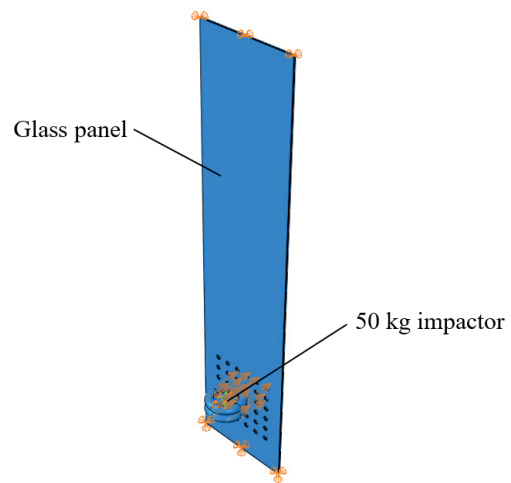
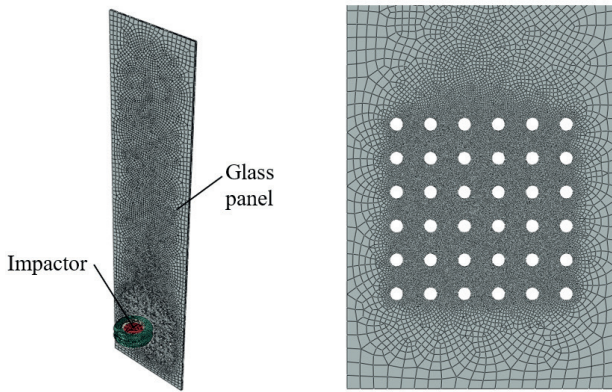


Fig. 8 Finite element model used for soft-body impact

shell elements allow for efficient modeling using only one element through the thickness of the element [13]. A convergence study was employed to determine optimum FE size of glass and interlayer. Different FE sizes around the holes (from 25 to 5 mm) were investigated while keeping the global element size of 40 mm. The results were studied by examining the relative change in output variable extrema with global maximum principal stress in glass  $\sigma_{1,max}$  as a base value. Fig. 10 shows results of the convergence study. It was concluded that the FE mesh converges to a sufficient degree at the FE size of 5 mm (relative change of global maximum principal stress in glass  $\sigma_{1,max}$  was less than 2 %). Final mesh pattern consisted of 88441 finite elements (Fig. 10).

Material properties of glass and interlayer are shown in Table 1. Glass was represented using linear elastic material properties according to [11]. In post-breakage state, reduced value of Young's modulus of fractured glass (in compression) was set based on previous studies [3].



**Fig. 9** Convergence of the FE model in terms of relative change of global maximum principal stress in glass

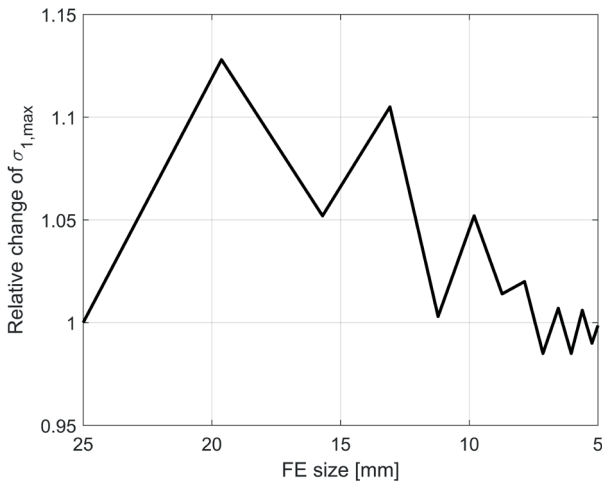


**Fig. 10** Convergence of the FE model in terms of relative change of global maximum principal stress in glass

**Table 1** Summary of material properties [11, 17, 3]

Material	Density [kN/m <sup>3</sup> ]	Elastic modulus [MPa]	Poisson's ratio [-]
Glass	25	70 000 (intact) 17 500 (fractured, in compression)	0.23
Interlayer	10	2.2 (5 min. load) 379.8 (20 ms load)	0.49

Due to the viscoelastic nature of the PVB interlayer, the mechanical response of a laminated glass element is substantially influenced by the duration of loading [14]. For static and dynamic loading, the value of Young's modulus was calculated with respect to [15, 16] for 5 min. and 20 ms load duration, respectively.

## 5 Results and discussion

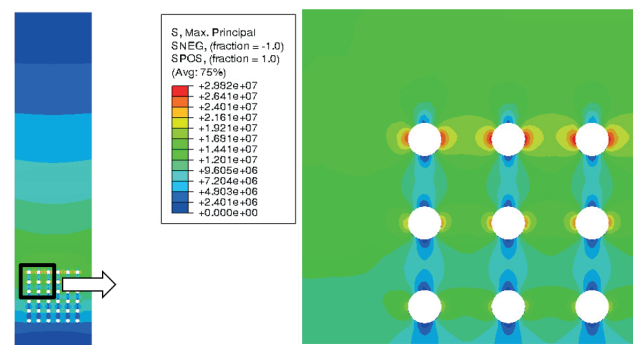
### 5.1 Static loading

Fig. 11 presents principal tensile stress map of the panel loaded with static barrier load. Clear influence of holes in the

glass resulting in stress concentrations can be observed. The stress around the holes (28.8 MPa) is approximately 60 % higher than the stress outside the perforated area.

Table 2 shows a comparison of experimental and numerical results in terms of horizontal displacement ( $\delta$ ) and vertical stress at specific positions of strain gauges ( $\sigma_{Y1}$ ,  $\sigma_{Y2}$ ,  $\sigma_{Y3}$ ). The table provides also predicted global values of maximum principal tensile stress ( $\sigma_{1,max}$ ) and maximum horizontal displacement ( $\delta_{max}$ ). For the purpose of the validation, the experimental results were considered as reference values. Table 2 shows that the numerical model is capable of predicting the values of stress and deflection with a reasonably good accuracy (differences less than 5 %). The maximum deflection of the panel (found in FE study) was approximately 4 % larger than the deflection predicted at the LVDT position. Similarly, the value of maximum (global) principal tensile stress in glass was found to be 52 % larger than the vertical stress simulated at the gauge position.

The value of maximum principal tensile stress in glass was checked against allowed values based on the characteristic strength of toughened glass 120 MPa [16] and the load duration factor  $k_{mod} = 0.77$  (for barrier loads). It was found that the utilization level of the panel under static load was 0.26. The maximum deflection was 24 % lower than the allowed value (43.8 mm) as specified by the standard [17].



**Fig. 11** Results of FE study: Map of maximum principal tensile stress in glass (figure shows tensile side of panel)

**Table 2** Experimental results (static barrier loading of 1 kN/m) for tested specimen and numerical FE predictions

	Values measured and predicted in specific locations				Global values predicted by FEM	
	$\delta$ [mm]	$\sigma_{Y1}$ [MPa]	$\sigma_{Y2}$ [MPa]	$\sigma_{Y3}$ [MPa]	$\sigma_{1,max}$ [MPa]	$\delta_{max}$ [mm]
EXP	30.22	20.72	15.40	14.28	-	-
FEM	28.90	18.99	15.42	14.84	28.82	33.34
FEM/EXP	0.96	0.92	1.00	1.04	-	-

### 5.2 Soft-body impact

Figs. 12 and 13 present results of soft-body impact simulations in terms of history of force ( $F$ ) in the pendulum and maximum principal tensile stress in glass ( $\sigma_{1,max}$ ), respectively. In addition, the figures show a comparison of results of the intact glass panel (continuous lines) and the panel with single glass ply fractured (dashed lines) subjected to soft-body impact released from 450 mm.

Dynamic response of a panel subjected to soft-body impact lasted much longer than the time of physical contact between the glass and the impactor. It can be noticed by comparing the histories of force and stress in glass. The maximum value of stress occurs approximately 10 ms later than the time when the force reaches its maximum.

The maximum force for the fractured model was approximately 8 % lower than for intact model for the same drop height (450 mm). It can be explained by the fact that the force highly depends on the stiffness of the panel. The fractured panel shows lower stiffness due to the reduced Young's modulus of glass for fractured ply. The fractured panel shows approximately 15 % higher value of maximum stress in comparison to the intact panel despite of lower force. This is due to the fact that in the laminated glass consisting of two plies with different Young's moduli the stiffer ply attracts more stress.

The results of the numerical studies are summarized in Table 3. The values of maximum principal tensile stress in glass was compared to the allowed values based on the characteristic strength of toughened glass 120 MPa [16] increased by a factor of 1.4 due to the increase of glass strength at high strain rates [2, 17]. Under soft-body impact the intact panel shows utilization level of 61 % for the highest impact energy (drop height of 900 mm). The fractured panel despite the lower stiffness presents the utilization level of 50 % for the reduced drop height (450 mm).

### 5.3 Reduced modelling

The soft-body simulations were re-run for a reduced panel without holes (Fig. 14). The global element size of the panel was kept 40 mm, which resulted in total number of finite elements of 9300, which is approximately 1/10 of the total number of finite elements of the model with holes.

To account for the increased stress around the holes, a stress concentration factor  $K_t$  for a single row of circular holes in infinite plate (Fig. 15) subjected to simple bending was considered [18].

The stress concentration factor  $K_t$  was calculated according to Eq. (2):

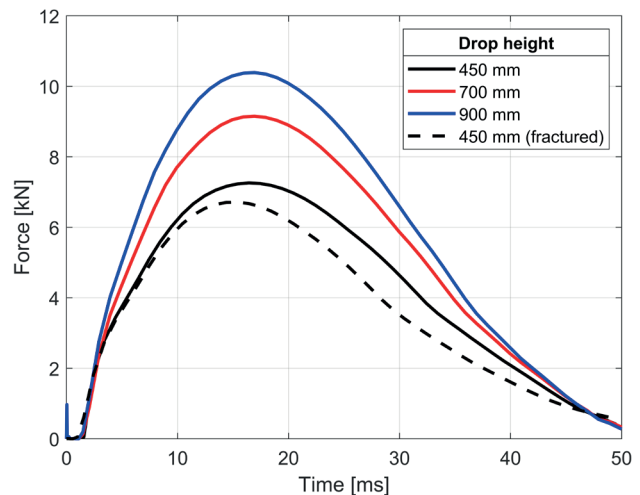


Fig. 12 Results of soft-body impact simulations (intact glass): Force vs. time

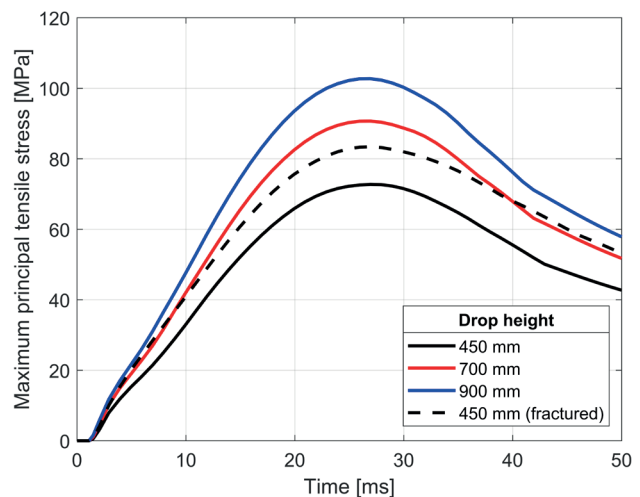


Fig. 13 Results of soft-body impact simulations (intact glass): Maximum principal tensile stress in glass vs. time

Table 3 Numerical results (soft-body impact)

Drop height [mm]	$F_{max}$ [kN]	$\sigma_{1,max}$ [MPa]	Allowed stress [MPa] [x,y]
Intact glass			
450	7.26	72.72	168.0
700	9.15	90.69	
900	10.39	102.7	
Fractured glass			
450	6.71	83.41	168.0

$$K_t = 1.787 - 0.060\left(\frac{d}{L}\right) - 0.785\left(\frac{d}{L}\right)^2 + 0.217\left(\frac{d}{L}\right)^3, \quad (2)$$

where  $d$  is the diameter of hole (50 mm) and  $L$  is the central spacing of the holes in an array (125 mm). For the panel with array of holes, the stress concentration factor  $K_t$  was 1.65.

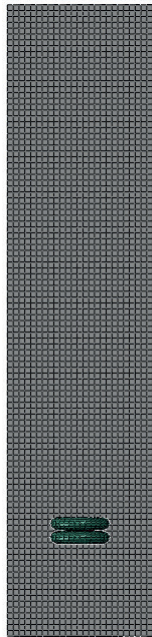


Fig. 14 Finite element mesh for reduced model (without holes)

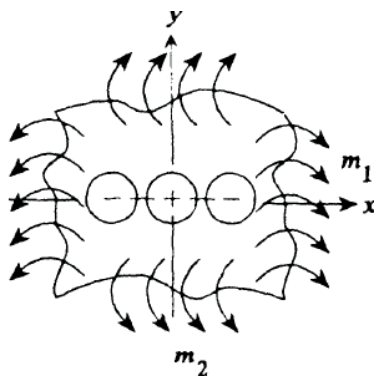


Fig. 15 Single row of circular holes in infinite plate [18]

Fig. 16 presents a comparison of results of soft-body impact simulations of the full model (with holes) and the reduced model without openings. The results of the reduced model were multiplied by the stress concentration factor  $K_r$ . The maximum value of principal tensile stress in glass for the reduced model overestimates the full model by only 5 %. This approach provides sufficient results and significantly reduces computation time of the impact analysis.

## 6 Conclusions

The paper presents a case study of a slender glass panel with complex geometry. It provides results of in-situ verification and results of numerical simulations that complement the experimental results. Based on the evaluation of the experiments and performed numerical studies the following conclusions can be drawn:

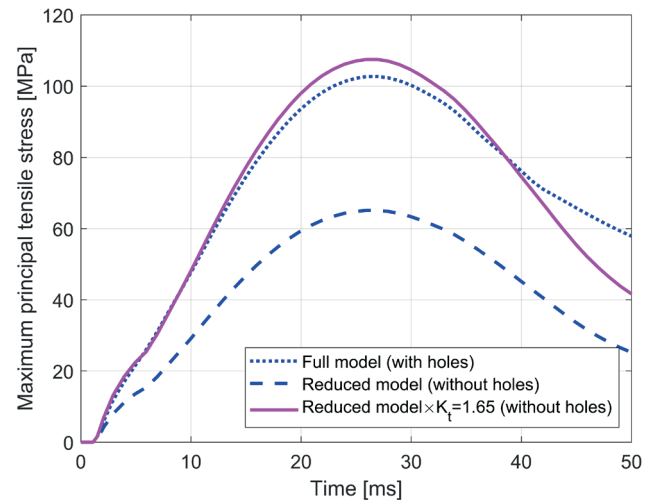


Fig. 16 Results of soft-body impact simulations (intact glass): Maximum principal tensile stress in glass vs. time

- The structural design of the glass panel was proven by experimental in-situ verification including static barrier loading and soft-body impact test of intact and in post-failure state. The results from the static loading test shows that under the loading of 1.0 kN/m, maximum stress and deflection are within acceptable limits. The soft body impact tests proved the safety of the panel in intact state and in in post-failure state (fractured glass).
- Nonlinear model developed is capable of producing accurate results and predicting the structural behavior of the glass panel under static barrier load (differences in comparison to experimental results were found to be less than 5 %).
- From the FE study on the impact behavior of the panel it is concluded that the glass panel is able to resistant soft-body impact from the double-tire impactor dropped from 900 mm. Pre-fractured panel shows approximately 15 % higher value of maximum stress in comparison to the intact panel despite of lower force.

## Acknowledgments

This work was supported by the on-going research project "Innovative solution for point-fixed laminated glass with improved capacity after glass fracture" (LIDER/34/0125/L-11/19/NCBR/2020) financed by The National Centre for Research and Development within the LIDER XI Programme.

## References

- [1] Weller, B., Härth, K., Tasche, S., Unnewehr, S. "Glass in Building. Principles, Applications, Examples", Birkhäuser, Berlin, Germany, 2009.
- [2] DIN "DIN 18004-4 Glass in Building – Design and construction rules – Part 4: Additional requirements for barrier glazing", German Institute for Standardization, Berlin, Germany, 2013.
- [3] Kozłowski, M. "Experimental and numerical assessment of structural behaviour of glass balustrade subjected to soft body impact", *Composite Structures*, 229, Article ID 111380, 2019. <https://doi.org/10.1016/j.compstruct.2019.111380>
- [4] Cwyl, M., Michalczyk, R., Grzegorzewska, N., Garbacz, A. "Predicting Performance of Aluminum - Glass Composite Facade Systems Based on Mechanical Properties of the Connection", *Periodica Polytechnica Civil Engineering*, 62(1), pp. 259–266, 2018. <https://doi.org/10.3311/PPci.9988>
- [5] Kozłowski, M., Kinsella, D., Persson, K., Kubica, J., Hulimka J. "Structural Analysis of Slender Glass Panel Subjected to Static and Impact Loading", *Challenging Glass Conference Proceedings*, 6, pp. 427–434, 2018. <https://doi.org/10.7480/cgc.6.2165>
- [6] Delincé, D., Callewaert, D., Belis, J., Van Impe, R. "Post-breakage behaviour of laminated glass in structural applications", In: *Proceedings of the Challenging Glass Conference on Architectural and Structural Applications of Glass*, Delft, The Netherlands, 2008, pp. 459–467. [online] Available at: <http://hdl.handle.net/1854/LU-416260>
- [7] Haldimann, M., Luible, A., Overend, M. "Structural Use of Glass", *International Association for Bridge and Structural Engineering (IABSE)*, Zurich, Switzerland, 2008. <https://doi.org/10.2749/sed010>
- [8] CEN "EN 1991-1-1 Eurocode 1: Actions on structures - Part 1-1: General actions - Densities, self-weight, imposed loads for buildings", European Committee for Standardization, Brussels, Belgium, 1991.
- [9] CEN "EN 12600 Glass in building. Pendulum test. Impact test method and classification for flat glass", European Committee for Standardization, Brussels, Belgium, 2002.
- [10] Hána, T., Eliášová, M., Sokol, Z. "Structural Performance of Double Laminated Glass Panels with EVA and PVB Interlayer in Four-Point Bending Tests", *International Journal of Structural Glass and Advanced Materials Research*, 2(1), pp. 164–177, 2018. <https://doi.org/10.3844/sgamrsp.2018.164.177>
- [11] CEN "EN 572–2 Glass in buildings - Basic soda lime silicate glass products", European Committee for Standardization, Brussels, Belgium, 2004.
- [12] Simulia "ABAQUS v. 6.14 Computer Software and Online Documentation", Dassault Systems, Providence, RI, USA, 2018. [online] Available at: <https://www.3ds.com/products-services/simulia/>
- [13] Fröling, M., Persson, K. "Computational Methods for Laminated Glass", *Journal of Engineering Mechanics*, 139(7), pp. 780–790, 2013. [https://doi.org/10.1061/\(ASCE\)EM.1943-7889.0000527](https://doi.org/10.1061/(ASCE)EM.1943-7889.0000527)
- [14] Quaglino, V., Cattaneo, S., Biolzi, L. "Numerical assessment of laminated cantilevered glass plates with point fixings", *Glass Structures & Engineering*, 5, pp. 187–204, 2020. <https://doi.org/10.1007/s40940-020-00119-5>
- [15] Belis J. L. I. F. "Kipsterkte van monolithische en gelamineerde glazen liggers (Buckling of monolithic and laminated glass beams)", PhD Thesis, Ghent University, 2005.
- [16] CEN "EN 16612 Glass in building. Determination of the lateral load resistance of glass panes by calculation", European Committee for Standardization, Brussels, Belgium, 2019.
- [17] Angelides, S. C., Talbot, J. P., Overend, M. "The effects of high strain-rate and in-plane restraint on quasi-statically loaded laminated glass: a theoretical study with applications to blast enhancement", *Glass Structures & Engineering*, 4, pp. 403–420, 2019. <https://doi.org/10.1007/s40940-019-00107-4>
- [18] Pilkey, W. D. "Formulas for stress, strain, and structural matrices", John Wiley & Sons, Hoboken, NJ, USA, 2005. <https://doi.org/10.1002/9780470172681>